Geomechanics and Engineering, *Vol. 13, No. 3 (2017) 431-446*
DOI: https://doi.org/10.12989/gae.2017.13.3.431

The effect of compression load and rock bridge geometry on the shear mechanism of weak plane

Vahab Sarfarazi [1], Hadi Haeri [*2] and Alireza Bagher Shemirani [3,4]

[1] *Department of Mining Engineering, Hamedan University of Technology, Hamedan, Iran*
[2] *Young Researchers and Elite Club, Bafgh Branch, Islamic Azad University, Bafgh, Iran*
[3] *Department of Civil Engineering, Sadra Institute of Higher Education, Tehran, Iran*
[4] *Department of Civil Engineering, Sharif University of Technology, Tehran, Iran*

(*Received June 18, 2016, Revised March 08, 2017, Accepted June 1, 2017*)

Abstract. Rock bridges in rock masses would increase the bearing capacity of Non-persistent discontinuities. In this paper the effect of ratio of rock bridge surface to joint surface, rock bridge shape and normal load on failure behaviour of intermittent rock joint were investigated. A total of 42 various models with dimensions of 15 cm × 15 cm × 15 cm of plaster specimens were fabricated simulating the open joints possessing rock bridge. The introduced rock bridges have various continuities in shear surface. The area of the rock bridge was 45 cm^2 and 90 cm^2 out of the total fixed area of 225 cm^2 respectively. The fabricated specimens were subjected to shear tests under normal loads of 0.5 MPa, 2 MPa and 4 MPa in order to investigate the shear mechanism of rock bridge. The results indicated that the failure pattern and the failure mechanism were affected by two parameters; i.e., the ratio of joint surface to rock bridge surface and normal load. So that increasing in joint area in front of the rock bridge changes the shear failure mode to tensile failure mode. Also the tensile failure change to shear failure by increasing the normal load.

Keywords: rock bridges; joint; normal loads; shear and tensile failure mode

1. Introduction

The behaviour of a rock mass is determined not only by the properties of the rock matrix, but mostly by the presence and properties of rock bridge and rock joint within the mass (Fig. 1). For example, for rock slope stability it is essential to know if and how existing fractures connect with each other or coalesce to form a continuous fracture surface. Also, persistence, orientation, and other properties of the fractures influence the deformability and strength of rock masses.

Therefore, a comprehensive study on the shear failure behaviour of jointed rock can provide a good understanding of both local and general rock instabilities, leading to an improved design for rock engineering projects. A number of experimental studies have been carried out to investigate the crack initiation, propagation and coalescence in the axial or biaxial test conditions (Vasarhelyi and Bobet 2000, Wong and Chau 1998, Shen 1993, Bobet and Einstein 1998, Germanovich *et al.* 1994). Two types of cracks can initiate from the tips of the two-dimensional pre-existing non-persistent discontinuity: tensile cracks that initiate at an angle from the tips of the flaw and

*Corresponding author, Assistant Professor, E-mail: h.haeri@bafgh-iau.ac.ir; haerihadi@gmail.com

Copyright © 2017 Techno-Press, Ltd.
http://www.techno-press.org/?journal=gae&subpage=7 ISSN: 2005-307X (Print), 2092-6219 (Online)

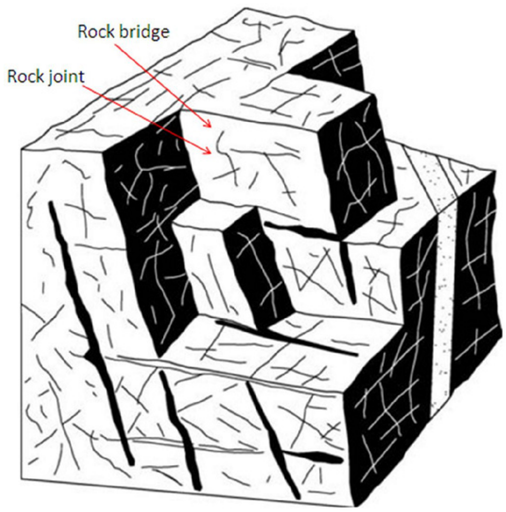

Fig. 1 Rock bridges in discontinuously-jointed rock

propagate in a stable manner towards the direction of maximum compression. Shear cracks that also initiate from the tips of the flaws and initially propagate in a stable manner.

The pattern of coalescence between two parallel crack in both modelling materials and natural rocks have been done in direct shear boxes (Lajtai 1969, Li *et al*. 1990). Lajtai (1969) performed direct shear test on natural rock specimens with two parallel slots, tensile wing cracks were found to first appear at the tips of horizontal joints, followed by the secondary shear cracks propagating towards the opposite joint. Also he observed that the failure mode changed with increasing normal stress; he suggested a composite failure envelope to describe the transition from the tensile strength of the intact material to the residual strength of the discontinuities. He thus recognized that maximum shear strength develops only if the strength of the solid material and the joints are mobilized simultaneously. Savilahti (Savilahti *et al*. 1990) did some further study on the specimens of jointed rock under direct shear tests where the joint separation varies in both horizontal and vertical directions and joint arrangement changes from non-overlapping to overlapping using modelling material. The coalescence patterns for the specimens indicated that the jointed rock failed in mixed mode for non-overlapping joint configuration and in tensile mode for overlapping joint form.

Wong *et al*. (2001) studied shear strength and failure pattern of rock-like models containing arrayed open joints in both modelling plaster material and natural rocks under direct shear tests. The results showed that failure pattern was mainly controlled by the joint separation while shear strength of jointed rock depended mostly on the failure pattern. Ghazvinian (Ghazvinian *et al*. 2007, 2008) made a thorough analysis of the shear behaviour of the rock-bridge based on the change in the rock-bridge persistency. The analysis shows that the failure mode and the failure mechanism are under the effect of the continuity of the rock-bridge. Also, a number of experimental studies have been carried out to investigate the crack initiation, propagation and coalescence in different loading condition (Yang *et al*. 2008, 2009, Fujii and Ishijima 2004, Wasantha *et al*. 2014, Zhang and Wong 2012, 2013, Bahaaddini 2013, Sarfarazi *et al*. 2014, Haeri *et al*. 2014, Haeri *et al*. 2015a, b, c, Haeri 2015a, b, c, Haeri and Sarfarazi 2016, Haeri *et al*. 2016, Sarfarazi and Haeri 2016, Sarfarazi *et al*. 2016). Since this rock segments have different configuration in shear surface and suffer different normal loading, therefore we come up with this question that weather the rock bridge configuration and normal loading influences the shear properties along the shear surface.

2. Experimental studies

The discussion of experimental studies is divided into four sections. The first section discusses the physical properties of a modelling material, the second section is describing the technique of preparing the jointed specimens, the third section is focused on the testing procedure and finally, the fourth section considers the general experimental observations and discussions.

2.1 Modelling material and its physical properties

The material used for this investigation is gypsum; the same material was used by Takeuchi (1991), Shen *et al*. (1995) and Bobet and Einstein (1998). Gypsum is chosen because, in addition to behave same as a weak rock, is an ideal model material which a wide range of brittle rocks can be represented; second, all the previous experiences and results can be incorporated and the earlier findings can be compared with the new ones; third, it allows to prepare a large number of specimens easily; Forth, repeatability of results. The samples are prepared from a mixture of the water and gypsum with a ratio of water to gypsum = 0.5.

Concurrent with the preparation of specimens and their testing, uniaxial compression and indirect tensile strengths of the intact material was also tested in order to control the variability of material. The uniaxial compressive strength (UCS) of the model material is measured on fabricated cylindrical specimens with 56 mm in diameter and 112 mm in length. The indirect tensile strength of the material is determined by the Brazilian test using fabricated solid discs 56 mm in diameter and 28 mm in thickness. The testing procedure of uniaxial compressive strength test and the Brazilian test complies with the ASTM D2938-86 (ASTM 1986) and ASTM C496-71, (ASTM 1971) codes respectively. The base material properties derived from unconfined compression and tensile test are as follows:

Average uniaxial compressive strength:	10 MPa
Average brazilian tensile strength:	1.2 MPa
Average Young's Modulus in compression:	3600 MPa
Average Poisson's ratio:	0.18

2.2 The technique in preparing the jointed specimens

The procedure developed by Bobet (Bobet and Einstein 1998) for preparing open non-persistent joints was used in this research with some modifications. The material mixture is prepared by mixing water and gypsum in a blender; the mixture is then poured into a steel mold with internal dimension of 15×15×15 cm. The mold consists of four steel sheets bolted together and of two PMMA plates, 1/6 inch thick, which are placed at the top and bottom of the mold. As shown in Fig. 2 the top plate has two rectangular openings used to fill the mold with the liquid gypsum mixture. The upper and the lower surfaces have slits cut into them. The width of slits is 0.5 mm (0.02 inch) and their length varies based on the length of the joints. The positions and

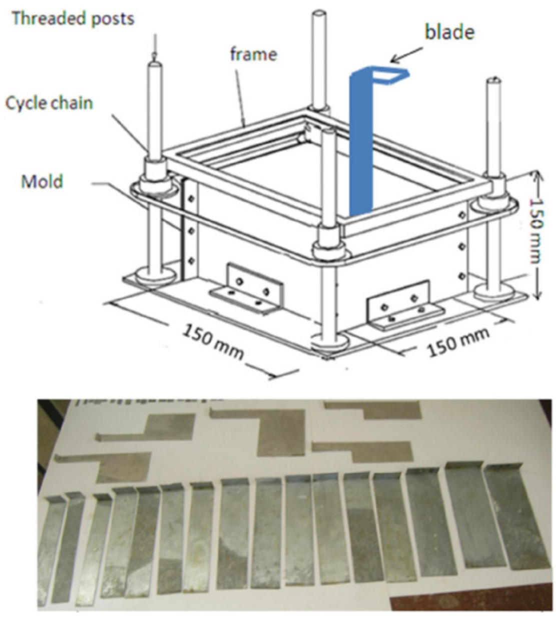

Fig. 2 Model used for the fabrication of the gypsum specimens

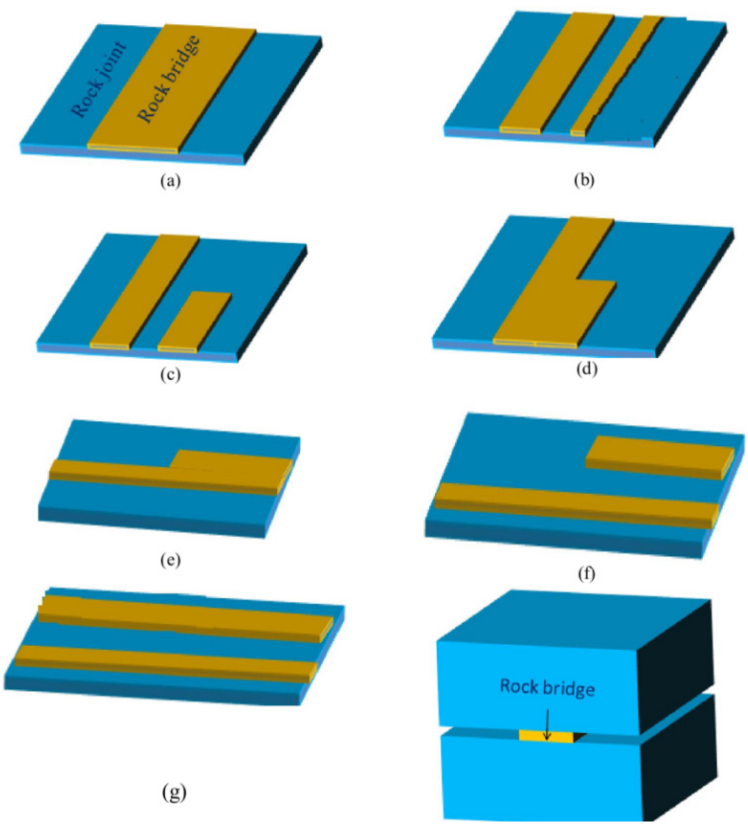

Fig. 3 The geometrical specifications of the various rock bridges; rock bridge area = 45 cm^2

number of the shims are predetermined to give a desired non-persistent joint. Through these slits, greased metallic shims are inserted through the thickness of the mold before pouring the gypsum. The mold with the fresh gypsum is vibrated and then stored at room temperature for 8 h afterward. The specimens un-molded and the metallic shims pulled out of the specimens; the grease on the shims prevents adhesion with the gypsum and facilitates the removal of the shims. As the gypsum seated and hardened, each shim leaves in the specimen an open joint through the thickness and perpendicular to the front and back of the specimen. Immediately after removing the shims, the front and back faces of the specimens are polished and the specimen is stored in laboratory for 4 days. At the end of the curing process, the specimens are tested. It does not appear that the pull out of the shims produces any damage through the joints. The aperture of joints is 0.5 mm, therefore the joint surface has not any effect on the failure mechanism.

The coplanar rock bridges have various configurations respect to shear loading direction and have occupied 45 cm^2, 90 cm^2 of the total shear surface (225 cm^2) respectively. The geometry and dimensions of non-persistent joints has shown in Fig. 3.

Based on the change in area of the rock-bridges, it is possible to define the Joint Coefficient, JC, as the ratio of joint surface that is in front of the rock-bridge to rock bridge surface. For example Figs. 4(a) and (b) compare two type of joint configuration in front of the rock bridge based on shearing direction. As can be seen from Fig. 4(a), all area of joint surfaces was distributed in front of the rock bridge but only dotted area of joint surface has distributed in front of the rock bridge in Fig. 2(b) and has important effect on the shearing process. Table 1 shows the amount of JC. In

Table 1 The amounts of the Joint Coefficients (JC) for various configurations

Rock bridge geometry	a	b	c	d	e	f	g
Rock bridge surface (cm^2)	45	45	45	45	45	45	45
Joint surface (cm^2)	180	180	160	180	60	60	0
JC	4	4	3.55	4	1.33	1.33	0
Rock bridge surface (cm^2)	90	90	90	90	90	90	90
Joint surface (cm^2)	135	135	105	135		45	0
JC	1.5	1.5	1.16	1.5		0.5	0

(a)

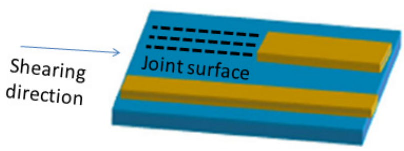

(b)

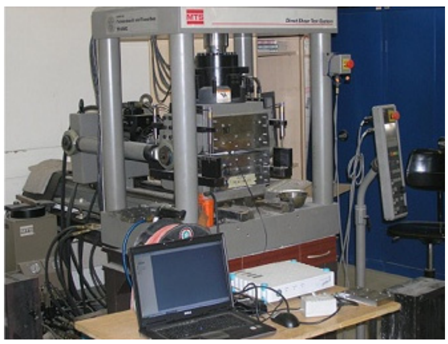

(c)

Fig. 4 (a) All area of joint surfaces has distributed in front of the rock bridge; (b) dotted area of joint surface has distributed in front of the rock bridge; (c) Direct shear test machine order to study the complete failure behaviour of rock bridges, from each configuration, two similar blocks were prepared and were tested under normal stresses of 0.5 MPa, 2 MPa and 4 MPa.

2.3 Testing program

A total of 42 direct shear tests were performed using direct shear test machine (Fig. 4). All tests are displacement-controlled. The tests were performed in such a way that the normal load 0.5 MPa, 1 MPa and 4 MPa, was applied to the sample and then shear load was adopted. Readings of shear loads, as well as the shear displacements are taken by a data acquisition system. Loading is carried out at a rate of the 0.002 mm/s.

The failure pattern was measured/observed after the test was completed. The shearing process of a discontinuous joint constellation begins, as one would expect, with the formation of new fractures which eventually transect the material bridges and lead to a through-going discontinuity.

3. Observations

By observing the failure surface after the tests, it is possible to investigate the effect of bridge configurations (or JC) and normal load on the failure mechanism of specimens. Figs. 5-11 show the tested models with rock bridge area of 45 cm^2 and 90 cm^2, respectively. The crack pattern is always a combination of only two types of cracks: wing cracks and shear cracks. Wing cracks start at the tip of the joints and propagate in a curvilinear path as the load increases. Wing cracks are tensile cracks and they grow in a stable manner, since an increase in load is necessary to lengthen the cracks. Shear cracks also initiate at tip of the joints and propagate in a stable manner.

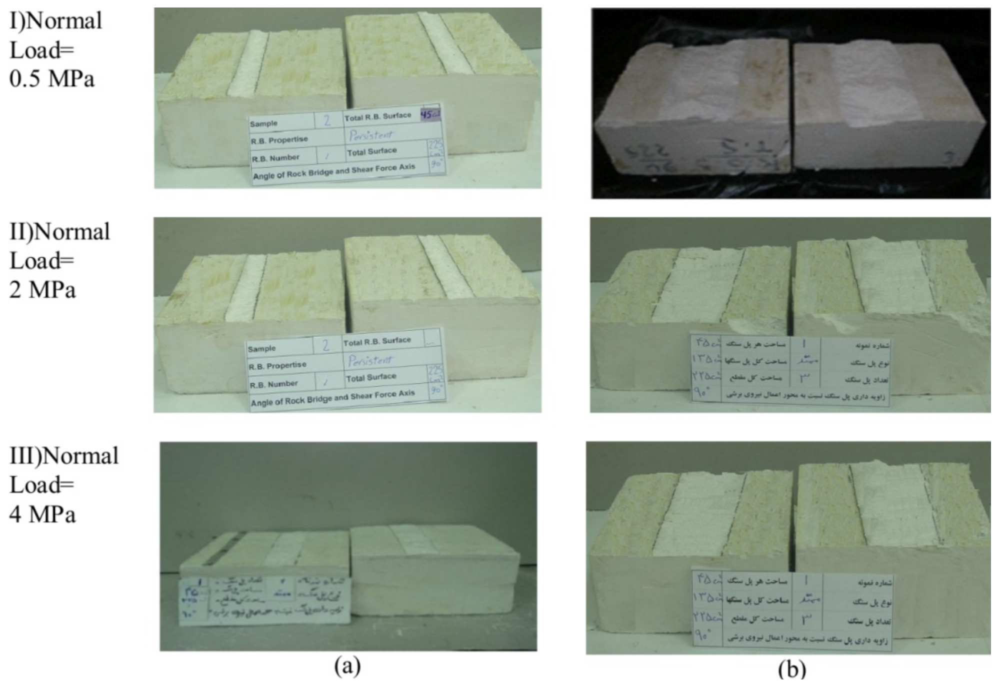

Fig. 5 Failure pattern in rock bridge configuration of "a" with area of (a) 45 cm^2; (b) 90 cm^2

I)Normal Load= 0.5 MPa

II)Normal Load= 2 MPa

III)Normal Load= 4 MPa

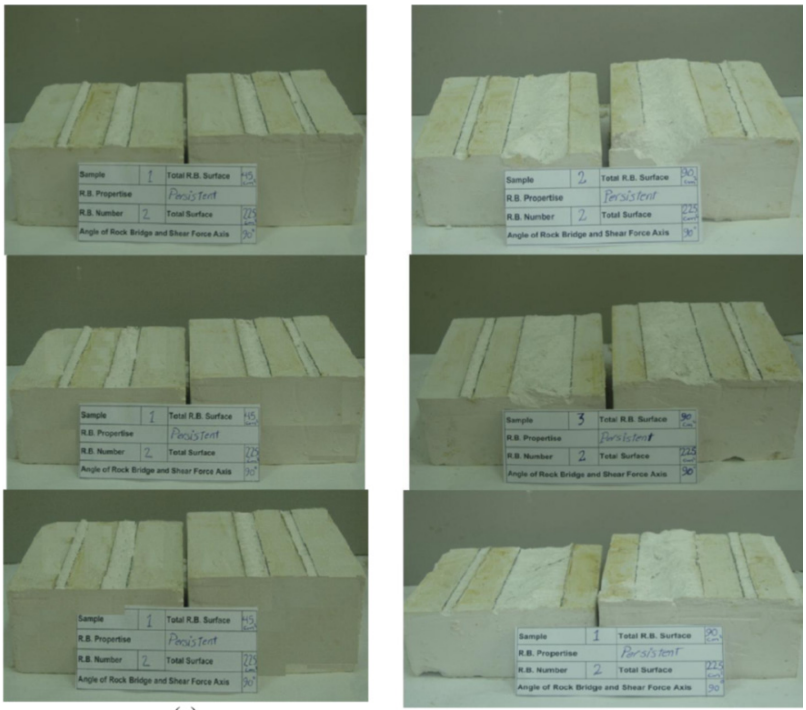

(a) (b)

Fig. 6 Failure pattern in rock bridge configuration of “b” with area of (a) 45 cm^2; (b) 90 cm^2

I)Normal Load= 0.5 MPa

II)Normal Load= 2 MPa

III)Normal Load= 4 MPa

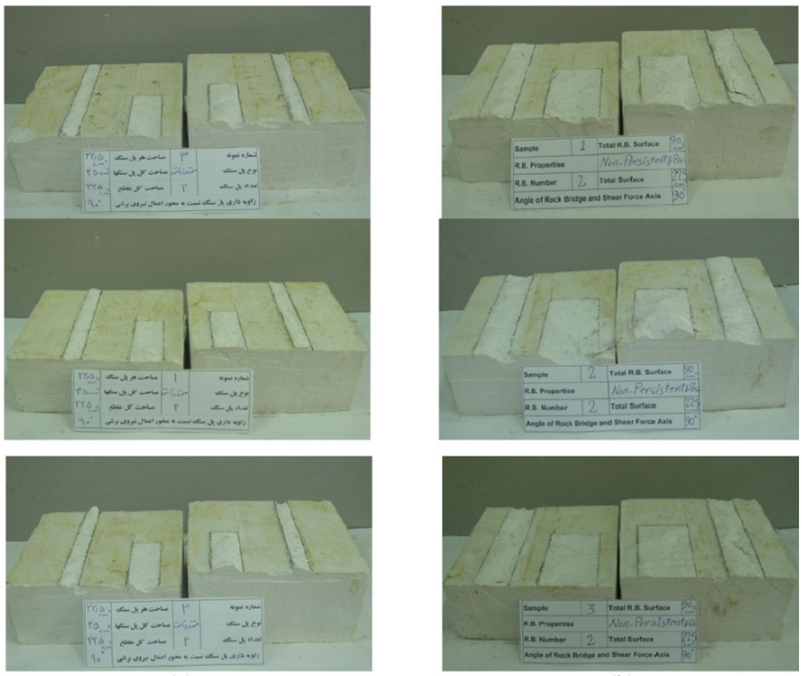

(a) (b)

Fig. 7 Failure pattern in rock bridge configuration of “c” with area of (a) 45 cm^2; (b) 90 cm^2

I)Normal Load= 0.5 MPa

II)Normal Load= 2 MPa

III)Normal Load= 4 MPa

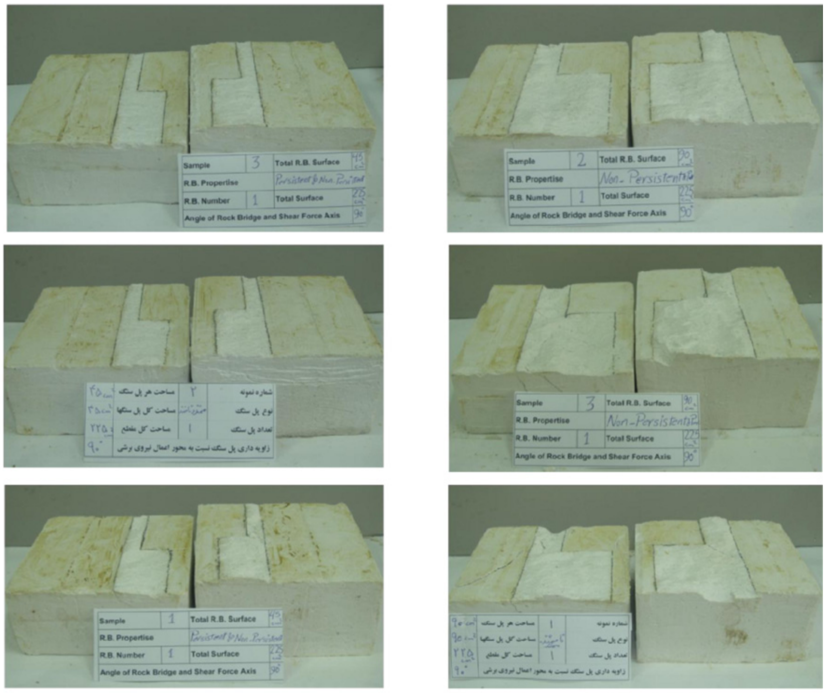

(a) (b)

Fig. 8 Failure pattern in rock bridge configuration of "d" with area of (a) 45 cm^2; (b) 90 cm^2

I)Normal Load= 0.5 MPa

II)Normal Load= 2 MPa

III)Normal Load= 4 MPa

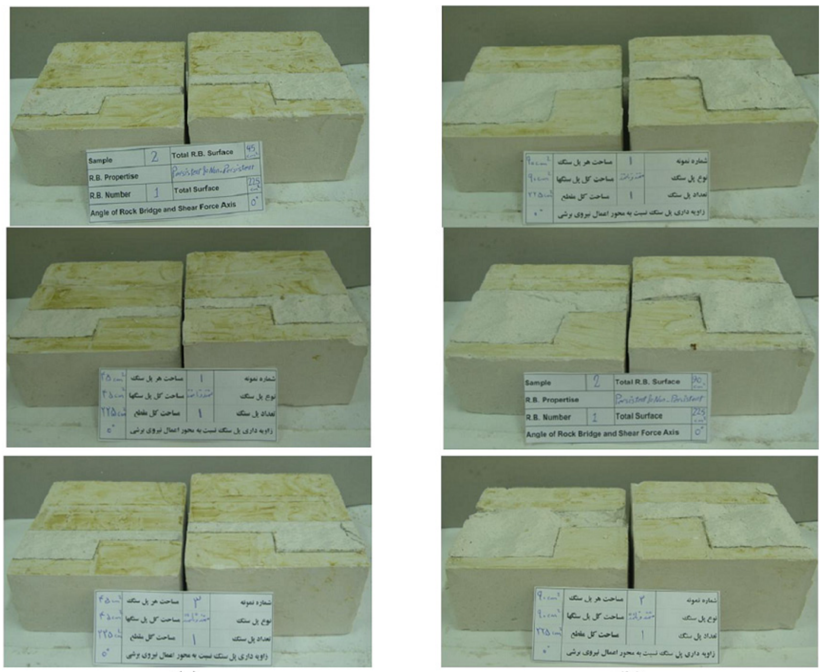

(a) (b)

Fig. 9 Failure pattern in rock bridge configuration of "e" with area of (a) 45 cm^2; (b) 90 cm^2

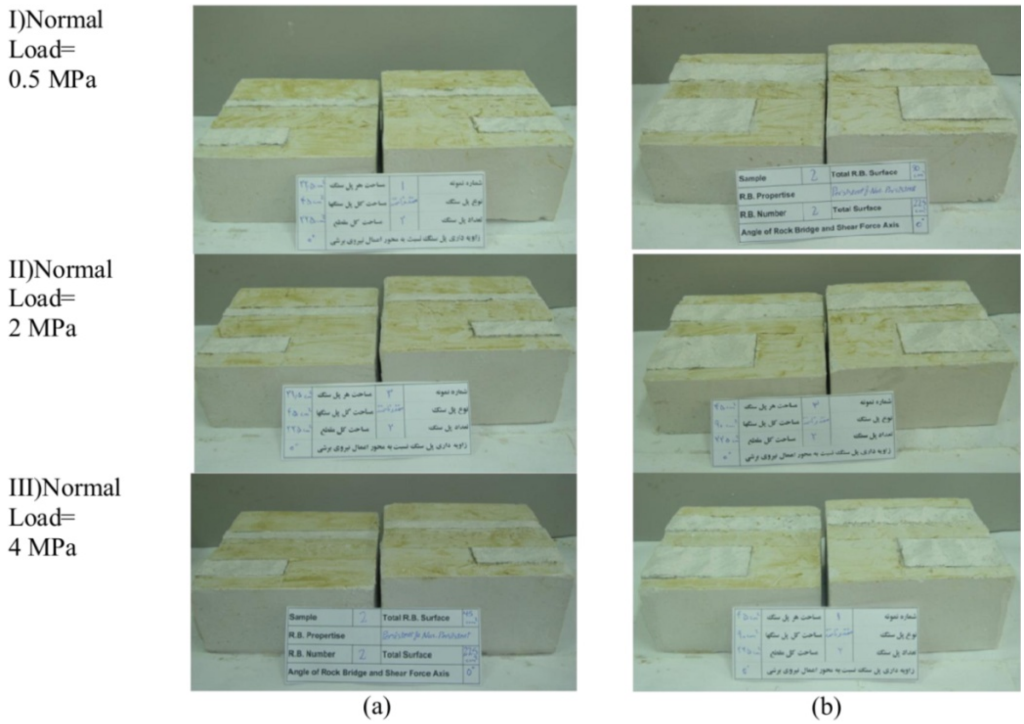

Fig. 10 Failure pattern in rock bridge configuration of "f" with area of (a) 45 cm^2; (b) 90 cm^2

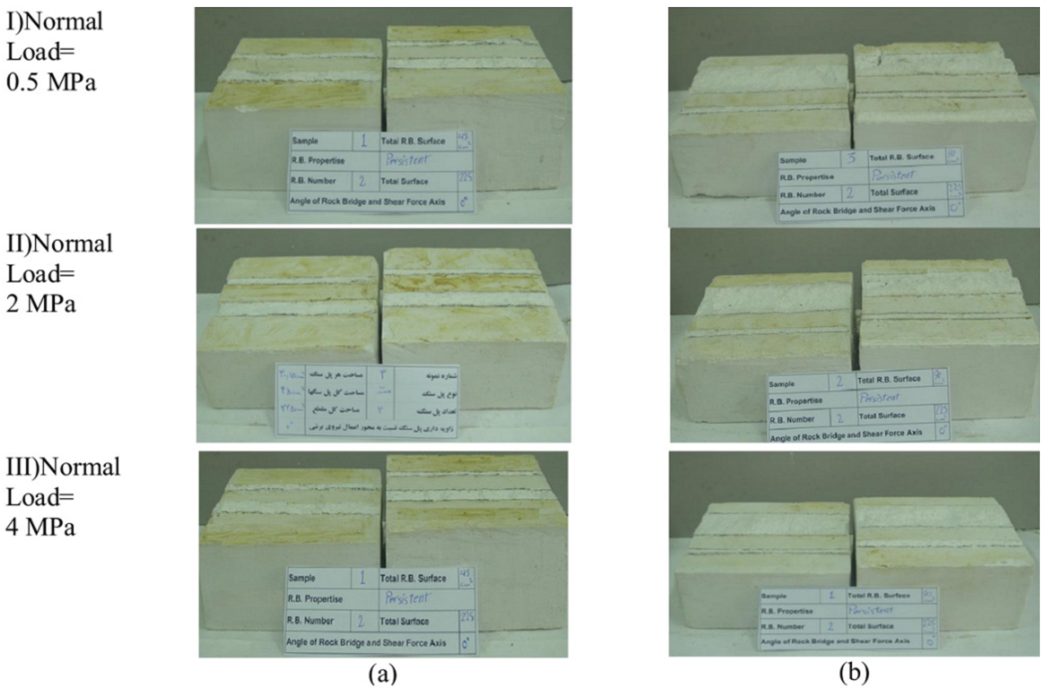

Fig. 11 Failure pattern in rock bridge configuration of "g" with area of (a) 45 cm^2; (b) 90 cm^2

3.1 The Failure pattern in rock bridges under normal stress of 0.5 MPa

Type I: The oval mode coalescence with two wing cracks

The oval mode coalescence, as defined in Figs. 5-8, a(I), occurs when JC >= 3.55. The wing cracks were initiated and propagated in curvilinear path that eventually aligned with the shear loading direction. The wing cracks propagate in a stable manner; and the external load needs to be increased for the cracks to propagate further. Each wing crack was initiated at the tip of the one joint and finally coalesced with the tip of the other joint. This coalescence left an oval core of intact material completely separated from the sample. The surface of failure is tensile because no crushed or pulverized materials and no evidence of shear movement were noticed. The wing cracks surfaces also had the same characteristics of tension surface. It is to be note that, when JC = 1.5 the oval mode coalescence appeared in samples consisting one, two and three rock bridges.

Type II: Coalescence with one arc wing crack

This coalescence, as defined in Figs. 9-10 a(I) and Figs. 5-8 b(I), occurred when 1.16 <= JC <= 3.55. In this configuration two arc wing cracks were initiated at the tip of the joints and propagated stably. The upper tensile crack can propagate through the intact portion area and finally coalesced with the inner tip of the other joint but the lower tensile crack develops for a short distance and then become stable so as not to coalesce with the tip of opposite joint. Examining the wing crack surface it was noticed that there was smooth and clean with no crushed or pulverized material and no evidence of shear displacement. These surface characteristics indicated that tensile stresses were responsible for the initiation and propagation of the wing cracks.

Type III: Coalescence with one semi arc wing crack

This coalescence, as defined in Fig. 11 a(I) and Figs. 9-10 b(I), occurred when JC <= 1.16. In this configuration the semi arc wing crack were initiated at the tip of the joint and propagated stably. The tensile crack can propagate through the intact portion area and finally coalesced with the inner tip of the other joint. Examining the wing crack surface it was noticed that there was smooth and clean with no crushed or pulverized material and no evidence of shear displacement. These surface characteristics indicated that tensile stresses were responsible for the initiation and propagation of the wing cracks.

3.2 The Failure pattern in rock bridges under normal stress of 2 MPa

Type II: Coalescence with one arc wing crack

This coalescence, as defined in Figs. 5-8, a(II), occurred when JC >= 3.55. In this configuration two arc wing cracks were initiated at the tip of the joints and propagated stably. The upper tensile crack can propagate through the intact portion area and finally coalesced with the inner tip of the other joint but the lower tensile crack develops for a short distance and then become stable so as not to coalesce with the tip of opposite joint. Examining the wing crack surface it was noticed that there was smooth and clean with no crushed or pulverized material and no evidence of shear displacement. These surface characteristics indicated that tensile stresses were responsible for the initiation and propagation of the wing cracks.

Type III: Coalescence with one semi arc wing crack

This coalescence, as defined in Figs. 9-10 a(II) and Figs. 5-8 b(II), occurred when 1.16 <= JC <= 3.55. In this configuration the semi arc wing crack were initiated at the tip of the joint and propagated stably. The tensile crack can propagate through the intact portion area and finally coalesced with the inner tip of the other joint. Examining the wing crack surface it was noticed that there was smooth and clean with no crushed or pulverized material and no evidence of shear displacement. These surface characteristics indicated that tensile stresses were responsible for the initiation and propagation of the wing cracks.

Type IV: Coalescence with mixed crack (shear/tensile)

This coalescence, as defined in Fig. 11 a(II) and Figs. 9-10 b(II) occurred when JC <= 1.16. At first the wing cracks were initiated at the tip of the joints and propagated stably. These wing cracks connect to each other by a shear crack. Examining the failure surface in near the joint tips, it was noticed that there was smooth and clean with no crushed or pulverized material and no evidence of shear displacement. These surface characteristics indicated that tensile stresses were responsible for the initiation and propagation of the wing cracks. Also the characteristics of the failure surface in the middle region were investigated. There was a significant amount of pulverized and crushed gypsum and traces of shear displacement, indicated that a shearing failure had taken place.

3.3 The Failure pattern in rock bridges under normal stress of 4 MPa

Type IV: Coalescence with mixed crack (shear/tensile)

This coalescence, as defined in Figs. 5-8 a(III) occurred when JC >= 3.55. At first the wing cracks were initiated at the tip of the joints and propagated stably. These wing cracks connect to each other by a shear crack. Examining the failure surface in near the joint tips, it was noticed that there was smooth and clean with no crushed or pulverized material and no evidence of shear displacement. These surface characteristics indicated that tensile stresses were responsible for the initiation and propagation of the wing cracks. Also the characteristics of the failure surface in the middle region were investigated. There was a significant amount of pulverized and crushed gypsum and traces of shear displacement, indicated that a shearing failure had taken place.

Type V: Coalescence with two shear cracks

This coalescence, as defined in Figs. 9-10 a(III) and Figs. 5-8 b(III), occurred when 1.16 <= JC <= 3.55. The mechanism of failure was characterized first by initiation of wing cracks followed by the initiation of secondary cracks at the tips of the joint segments. Then the two wing cracks were stopped while the two secondary cracks were propagated to meet each other at a point in the bridge area. The propagation and coalescence of the secondary cracks brought rock bridges to failure. The shear failure surface is in a wavy mode. Inspection of the surface of the cracks producing coalescence reveals the presence of many small kink steps, crushed gypsum and gypsum powder, which suggested coalescence through shearing.

Type IV: Coalescence with pure shear crack

This coalescence, as defined in Fig. 11 a(III) and Figs. 9-10 b(III) occurred when JC <= 1.16. The mechanism of failure was characterized by initiation of secondary cracks at the tips of the joint segments. Two secondary cracks were propagated to meet each other at a point in the bridge area. The propagation and coalescence of the secondary cracks brought rock bridges to failure. The shear failure surface is in a wavy mode. Inspection of the surface of the cracks producing coalescence reveals the presence of many small kink steps, crushed gypsum and gypsum powder, which suggested coalescence through shearing.

4. Description of the shear stress versus shear displacement curves

4.1 The effect of rock bridge shape on the shear stress versus shear displacement curve

Figs. 12(a) and (b) shows shear stress versus shear displacement curves for rock bridge area of 45 cm^2 under two normal load of 0.5 MPa and 4 MPa, respectively. Also, Figs. 13(a) and (b) shows shear stress versus shear displacement curves for rock bridge area of 90 cm^2 under two normal load of 0.5 MPa and 4 MPa, respectively. The rock bridges have various configurations. In fixed normal load, the inclination of the curve or shear stiffness of rock bridge, was decreased with increasing the JC (Figs. 12 and 13(a) and (b)). For example sample a, which has highest JC, i.e., 4 and 1.5 for rock bridge area of 45 cm^2 and 90 cm^2, respectively, show lowest shear stiffness. But sample g which has highest JC (0 for rock bridge area of 45cm^2 and 90 cm^2, respectively) has highest shear stiffness. In fact the stress concentration a tip of the joint was decreased by decreasing the JC so interlocking force between the grains was increased. This leads to increasing in the shear stiffness of rock bridge.

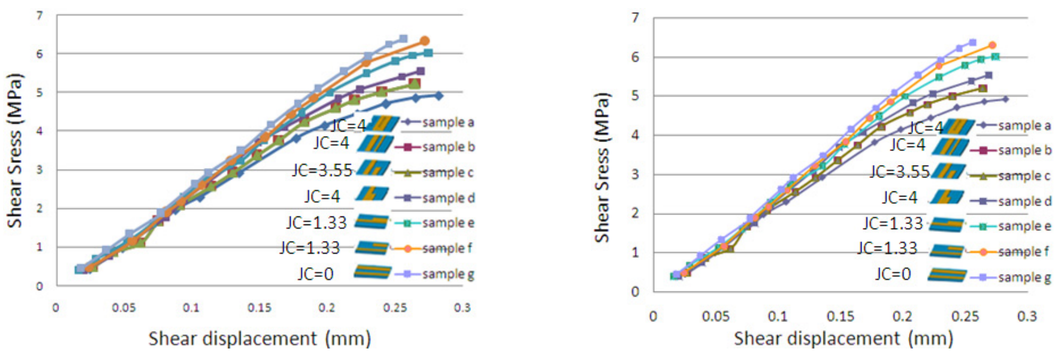

(a) (b)

Fig. 12 Shear stress versus shear displacement curves for the models under two normal load of: (a) 0.5 MPa; (b) 4 MPa; rock bridge area = 45 cm^2

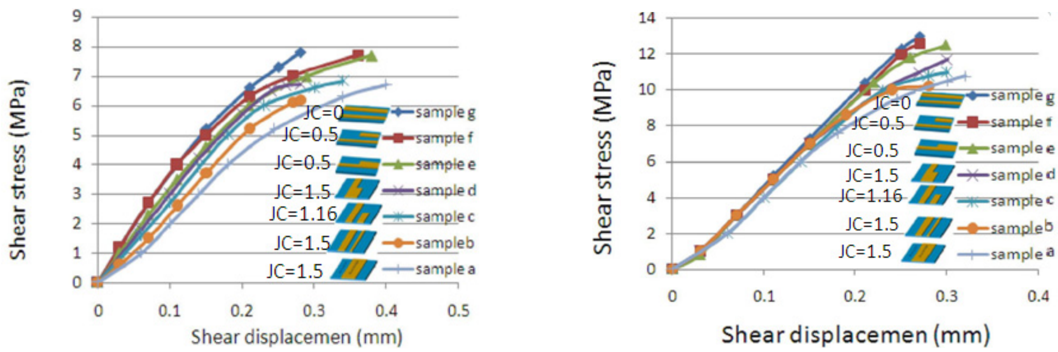

(a) (b)

Fig. 13 Shear stress versus shear displacement curves for the models under two normal load of: (a) 0.5 MPa; (b) 4 MPa; rock bridge area = 90 cm^2

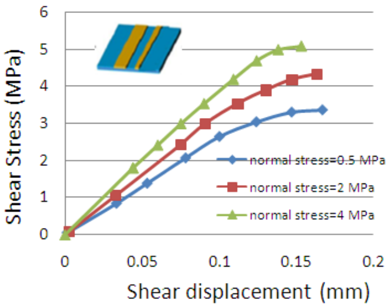

(a)

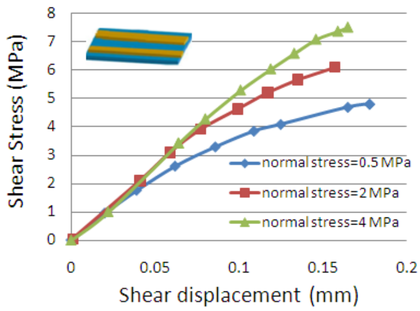

(b)

Fig. 14 Shear stress versus shear displacement curves for the models under different normal load: (a) latitudinal rock bridge; (b) longitudinal rock bridge; rock bridge area = 45 cm^2

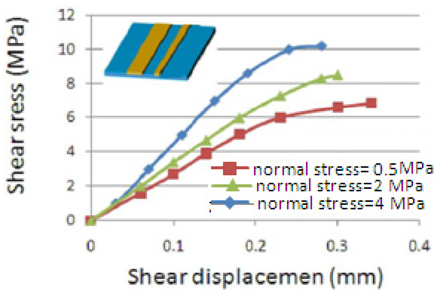

(a)

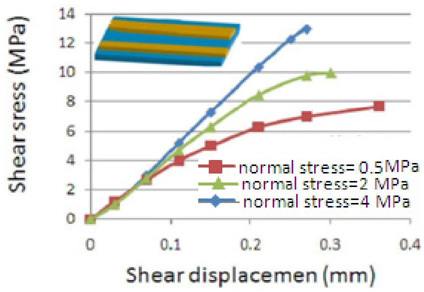

(b)

Fig. 15 Shear stress versus shear displacement curves for the models under different normal load: (a) latitudinal rock bridge; (b) longitudinal rock bridge; rock bridge area = 90 cm^2

4.2 The effect of normal load on the shear stress versus shear displacement curve

Figs. 14(a) and (b) shows shear stress versus shear displacement curves for two different configuration of rock bridge with area of 45 cm^2. Figs. 15(a) and (b) shows shear stress versus shear displacement curves for two different configuration of rock bridge with area of 90 cm^2. The stiffness was shown for three different normal loads. The inclination of the curve, or shear stiffness of rock bridge, was increased with increasing the rock normal load (Figs. 13(a) and (b)). In fact, the compaction of rock bridge was increased by increasing the normal load so interlocking force between the grains was increased. This leads to increasing the shear stiffness of rock bridge.

5. Shear strength of samples consisting various rock bridge configurations

Fig. 16 shows shear strength versus rock bridge configuration for rock bridge area of 45 cm^2. Also, Fig. 17 shows shear strength versus rock bridge configuration for rock bridge area of 45 cm^2. Shear strengths were registered for three different normal loads. Sample a, b and d has lowest shear strength. In this configuration, JC has maximum value, i.e., 1.5 for rock bridge area of 90 cm^2 (Table 1). Whereas the highest joint surface has occupied the shear surface therefore high stress consecration occurred at tip of the joint. This leads to decreasing in the shear strength.

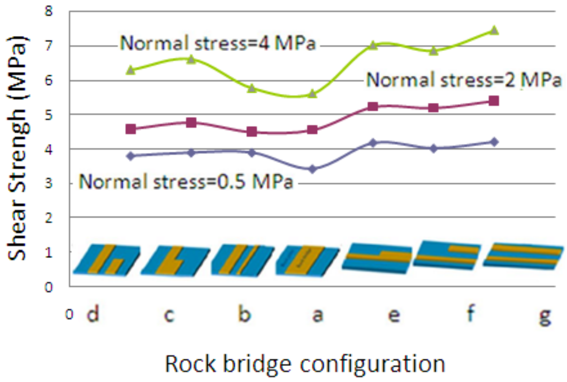

Fig. 16 Shear strength versus rock bridge configuration in three different normal stresses; rock bridge area = 45 cm^2

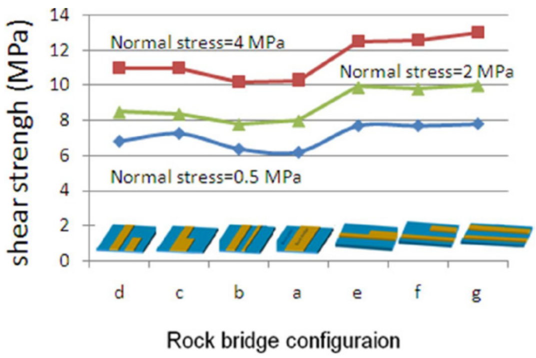

Fig. 17 Shear strength versus rock bridge configuration in three different normal stresses; rock bridge area = 90 cm^2

Sample g has highest shear strength. In this configuration, JC has minimum value, i.e., 0 for rock bridge area of 90 cm^2 (Table 1). Whereas the joint has disappeared in shear surface therefore no stress consecration occurred along the shear surface. This leads to increasing in shear strength. It's to be note that the shear resistance along the failure surface increase with increasing he normal stress.

6. Conclusions

The shear behaviour of rock-like specimens containing various configurations of rock bridges with different areas has been investigated under three different normal stresses through direct shear test. The results show that both of the failure pattern and failure mechanism are mostly influenced by JC and normal stress. While both of the shear strength and shear stiffness are closely related to the ratio of rock bridge surface to joint surface and normal stress. The following conclusions can be drawn from the experimental tests:

(1) The shear failure mode in the rock-bridge changes to the tensile failure mode by increasing in the Joint Coefficient.

(2) The shear failure mode in the rock-bridge changes to the tensile failure mode by decreasing the normal load.
(3) In the fixed area of the rock-bridge, with decreasing in Joint Coefficient, a very high stress concentration (tensile and shear stress) was established at tip of the joints due to the interaction between the joint tips.
(4) The shear failure mode in the rock-bridge changes to the tensile failure mode.
(5) The shear strength is closely related to the rock bridge failure pattern and failure mechanism, so that in the fixed area of the rock-bridge, the rock-bridge resistance reduced with change in failure mode from shear to tensile.
(6) For the fixed area of the rock bridge, the shear resistance along the failure surface increase with decreasing the JC.
(7) For the fixed area of the rock bridge, the shear resistance along the failure surface increase with increasing the normal stress.

References

ASTM (1986), Test method for unconfined compressive resistance of intact rock core specimens; ASTM designation D2938-86.

ASTM (1971), Standard method of test for splitting tensile resistance of cylindrical concrete specimens; ASTM designation C496-71.

Bobet, A. and Einstein, H.H. (1998), "Fracture coalescence in rock-type materials under uniaxial and biaxial compression", *Int. J. Rock Mech., Min. Sci. Geomech. Abstract*, **35**(7), 863-889.

Bahaaddini, M. (2013), "Numerical investigation of the effect of joint geometrical parameters on the mechanical properties of a non-persistent jointed rock mass under uniaxial compression", *Comput. Geotech.*, **49**, 206-225.

Fujii, Y. and Ishijima, Y. (2004), "Consideration of fracture growth from an inclined slit and inclined initial fracture at the surface of roc k and mortar in compression", *Int. J. Rock Mech. Min. Sci.*, **41**(6), 1035-1041.

Germanovich, L.N., Salganik, R.L., Dyskin, A.V. and Lee, K.K. (1994), "Mechanisms of brittle fracture of rocks with multiple pre-existing cracks in compression", Pure Appl. Geophys., **143**(1/2/3), 117-149.

Ghazvinian, A., Nikudel, M.R. and Sarfarazi, V. (2007), "Effect of rock bridge continuity and area on shear behavior of joints", *Proceedings of the 11th Congress of the International Society for Rock Mechanics*, Lisbon, Portugal, July, pp. 518-522.

Ghazvinian, A., Nikudel, M.R. and Sarfarazi, V. (2008), "Determination of sliding path in rock slopes containing coplanar non-persistent open discontinuity", *World Appl. Sci. J.*, **3**(4), 577-589.

Haeri, H. (2015a), "Experimental crack analysis of rock-like CSCBD specimens using a higher order DDM", *Comput. Concrete*, **16**(6), 881-896.

Haeri, H. (2015b), "Influence of the inclined edge notches on the shear-fracture behavior in edge-notched beam specimens", *Comput. Concrete*, **16**(4), 605-623.

Haeri, H. (2015c), "Propagation mechanism of neighboring cracks in rock-like cylindrical specimens under uniaxial compression", *J. Min. Sci.*, **51**(3), 487-496.

Haeri, H. and Sarfarazi, V. (2016), "The effect of micro pore on the characteristics of crack tip plastic zone in concrete", *Comput. Concrete, Int. J.*, **17**(1), 107-112.

Haeri, H., Shahriar, K., Marji, M.F. and Moarefvand, P. (2014), "Investigating the fracturing process of rock-like Brazilian discs containing three parallel cracks under compressive line loading", *Strength of Mater.*, **46**(3), 133-148.

Haeri, H., Khaloo, K. and Marji, M.F. (2015a), "Experimental and numerical analysis of Brazilian discs with multiple parallel cracks", *Arab. J. Geosci.*, **8**(8), 5897-5908.

Haeri, H., Marji, M.F. and Shahriar, K. (2015b), "Simulating the effect of disc erosion in TBM disc cutters by a semi-infinite DDM", *Arab. J. Geosci.*, **8**(6), 3915-3927.

Haeri, H., Shahriar, K., Marji, M.F. and Moarefvand, P. (2015c), "On the HDD analysis of micro crack initiation, propagation, and coalescence in brittle materials", *Arab. J. Geosci.*, **8**(5), 2841-2852.

Haeri, H., Sarfarazi, V. and Lazemi, H. (2016), "Experimental study of shear behavior of planar non-persistent joint", *Comput. Concrete*, *Int. J.*, **17**(5), 639-653.

Lajtai, E.Z. (1969), "Strength of discontinuous rocks in direct shear", *Geotechnique*, **19**(2), 218-233.

Li, C., Stephansson, O. and Savilahti, T. (1990), "Behaviour of rock joints and rock bridges in shear testing", *Proceedings of International Symposium on Rock Joints*, (N. Barton and O. Stephansson Ed.), Loen, Norway, June, pp. 259-266.

Sarfarazi, V. and Haeri, H. (2016), "Effect of number and configuration of bridges on shear properties of sliding surface", *J. Min. Sci.*, **52**(2), 245-257.

Sarfarazi, V., Ghazvinian, A., Schubert, W., Blumel, M. and Nejati, H.R. (2014), "Numerical simulation of the process of fracture of echelon rock joints", *Rock Mech. Rock Eng.*, **47**(4), 1355-1371.

Sarfarazi, V., Haeri, H. and Khaloo, A. (2016), "The effect of non-persistent joints on sliding direction of rock slopes", *Comput. Concrete*, *Int. J.*, **17**(6), 723-737.

Savilahti, T., Nordlund, E. and Stephansson, O. (1990), "Shear box testing and modeling of joint bridge", *Proceedings of International Symposium on Shear Box Testing and Modeling of Joint Bridge Rock Joints*, Loen, Norway, June, pp. 295-300.

Shen, B. (1993), "The mechanics of fracture coalescence in compression experimental study and numerical simulation", *Eng. Fract. Mech.*, **51**(1), 73-85.

Shen, B., Stephansson, O., Einstein, H.H. and Ghahreman, B. (1995), "Coalescence of fractures under shear stress experiments", *J. Geophy. Res.*, **100**(6), 5975-5990.

Takeuchi, K. (1991), "Mixed-mode fracture initiation in granular brittle materials", M.S. Thesis; Massachusetts Institute of Technology, Cambridge, MA, USA.

Vasarhelyi, B. and Bobet, A. (2000), "Modeling of crack initiation, propagation and coalescence in uniaxial compression", *Rock Mech. Rock Eng.*, **33**(2), 119-139.

Wasantha, P.L.P., Ranjith, P.G. and Shao, S.S. (2014b), "Energy monitoring and analysis during deformation of bedded sandstone: Use of acoustic emission", *Ultrasonic*, **54**(1), 217-226.

Wong, R.H.C. and Chau, K.T. (1998), "Crack coalescence in a rock-like material containing two cracks", *Int. J. Rock Mech. Min. Sci.*, **35**(2), 147-164.

Wong, R.H.C., Leung, W.L. and Wang, S.W. (2001), "Shear strength study on rocklike models containing arrayed open joints", In: *Rock Mechanics in the National Interest*, (D. Elsworth, J.P. Tinucci, K.A. Heasley Ed.), Swets & Zeitlinger Lisse, pp. 843-849. ISBN: 90-2651-827-7.

Yang, S.Q., Jiang, Y.Z., Xu, W.Y. and Chen, X.Q. (2008), "Experimental investigation on strength and failure behavior of pre-cracked marble under conventional triaxial compression", *Int. J. Solids Struct.*, **45**(17), 4796-4819.

Yang, S.Q., Dai, Y.H., Han, L.J. and Jin, Z.Q. (2009), "Experimental study on mechanical behavior of brittle marble samples containing different flaws under uniaxial compression", *Eng. Fract. Mech.*, **76**(12), 1833-1845.

Zhang, X.P. and Wong, L.N.Y. (2012), "Cracking process in rock-like material containing a single flaw under uniaxial compression: A numerical study based on parallel bonded-particle model approach", *Rock Mech. Rock Eng.*, **45**(5), 711-737.

Zhang, X.P. and Wong, R.H.C. (2013), "Crack initiation, propagation and coalescence in rock-like material containing two flaws: A numerical study based on bonded- particle model approach", *Rock Mech. Rock Eng.*, **46**(5), 1001-1021.

CC